THE EFFECTS OF SMALL ADDITION OF MOLYBDENUM ON THE STRUCTURE AND PROPERTIES OF LOW CARBON STRUCTURAL STEELS

By

Mohammad Abidur Rahman

A Thesis submitted to the Department of Materials and Metallurgical Engineering, Bangladesh University of Engineering and Technology (BUET), in partial fulfillment of the requirements for the Degree of Master of Science in Engineering (Metallurgical).

September, 1999

Bangladesh University of Engineering and Technology (BUET)
Dhaka, Bangladesh

DECLARATLON

This is to certify that this research work has been carried out by the author under the supervision of Dr. Md. Mohar Ali, Professor, Department of Materials and Metallurgical Engineering, Bangladesh University of Engineering and Technology (BUET), Dhaka and it has not been submitted elsewhere for the award of any other degree or diploma.

Countersigned

Md. Mohar Ali

Supervisor

M. A. Rahman

Signature of the author

The undersigned examiners appointed by the Committee of Advanced Studies and Research (CASR) hereby recommend to the Department of Materials and Metallurgical Engineering of Bangladesh University of Engineering and Technology (BUET), Dhaka, the acceptance of the thesis entitled " **THE EFFECTS OF SMALL ADDITION OF MOLYBDENUM ON THE STRUCTURE AND PROPERTIES OF LOW CARBON STRUCTURAL STEELS** " submitted by Mohammad Abidur Rahman, B. Sc. Engg. (Metallurgical) in partial fulfillment of the requirements for the degree of Master of Science in Engineering (Metallnrgical).

1. Md. Mohar Ali 29.9.99
   Prof. Dr. Md. Mohar Ali — Chairman
   Department of Materials and Metallurgical Engineering — (Supervisor)
   BUET, Dhaka

2. E. Haque 29.9.99
   Head — Member
   Department of Materials and Metallurgical Engineering
   BUET, Dhaka

3. N. Haque 29.9.99
   Prof. Dr. Md. Nasrul Haque — Member
   Department of Materials and Metallurgical Engineering
   BUET, Dhaka

4. [signature] 29.9.99
   Prof. Dr. Md. Serajul Islam — Member
   256/2/A, Sultanganj — (External)
   Rayer Bazar, Dhaka

ACKNOWLEDGEMENTS

The author would like to express his sincere gratitude and profound indebtedness to the thesis supervisor Dr. Md Mohar Ali, Professor, Department of Materials and Metallurgical Engineering, Bangladesh University of Engineering and Technology (BUET), Dhaka for his inspiring guidance, constant advice, encouragement and kind help in carrying out the research work as well as in preparing this thesis.

The author wishes to extend his thanks to Dr. Ehsanul Haque, Professor and Head, Department of Materials and Metallurgical Engineering (BUET), for providing the laboratory facilities.

The author also would like to give thanks to Dr. Md. Serajul Islam, Professor (Retired), Department of Materials and Metallurgical Engineering (BUET), for his continuous help in every step of the work, especially in repairing induction furnace.

The author is grateful to Mr. Fazlul Haque Bhuiyan, Senior Foundry Instructor, Mr. Md. Yusuf Khan, Sub-Assistant Engr., Babu Binoy Bhushan Shah, Senior Laboratory Instructor, Md. Ashikur Rahman, Senior Laboratory Instructor, Md Shamsul Alam, Craft Instructor, Md Feroz Hamid Khan, Laboratory Instructor and Md. Hanif, of the Department of Materials and Metallurgical Engineering for their kind help at different stages of this project

Finally the author express his gratitude to his parents and well wishes for their continued inspiration throughout the period of this research work.

The Author

ABSTRACT

An attempt has been made to study the effects of molybdenum and nickel on the structure and properties of 0·11% carbon steels. The austenite grain coarsening behaviour of these steels have been first studied. The carburization technique has been adopted to reveal the prior austenite grain boundaries.

It is observed from the variation of prior austenite grain size with temperature in the steels indicates that the undissolved particles molybdenum carbide, $M0_2C$, refine the austenite grain size at all temperatures, but the effect decreasing with increasing temperature. Nickel does not produce any austenite grain refinement In presence of nickel, particles of Mo_2C are less effective than particles of Mo_2C in the absence of nickel in the refinement of austenite grain size.

The standard tensile specimens made from heat-treated steel bars at temperatures corresponding to a common austenite grain size cooled at four different rates were tested to obtain data on tensile properties. The ferrite grain size of the steels after transformation suggests that the precipitating particles of Mo_2C have no effect in ferrite grain size refinement, while nickel refines the ferrite grain size.

At all the cooling rates, Mo_2C particles increase yield strength. A reduction in cooling rate resulted in reduced strengthening because of particle coarsening. In presence of nickel, the contribution of Mo_2C to yield strength is more than that of Mo_2C in the absence of nickel. Nickel in solution also contributes to yield strength.

The cooling rate has a little effect on the volume fraction of pearlite. It affects the ductility of the steels. Ductility is found to increase with decreasing cooling rates in the presence of nickel and molybdenum while the ductility is found to increase with increasing cooling rates if the steel is merely plain carbon. Both molybdenum and nickel decrease the ductility of low carbon steel, but molybdenum is more harmful than nickel

CONTENTS

CHAPTER 1

INTRODUCTION

In the early days C-Mn steels were used for structural purpose. The designs with these early structural steels for building, line pipe etc. were based only on tensile strength Little importance was given to toughness, weldability and formability. The cheapest alloying element, carbon, was used to achieve the tensile strength required. These steels although of the ferrite-pearlite type, were relatively high in carbon content, usually of the order of 0.3%. However, to widen the scope of steels to other structural applications, e.g. offshore structures, where welding is the principal fabrication process, it becomes more relevant to select steels on the basis of their post-weld properties[1]. When welding became more widely introduced as a fabrication process, structural failures in the steels then available occurred within the heat-affected zone [HAZ] owing to the formation of unfavourable micro-constituents that demanded an improvement in toughness and weldability. This led to the development of low-carbon steel to give better weldability and lower impact transition temperature. At the same time, it was realized that yield strength is a better design criterion than ultimate tensile strength. Advances in engineering design demand these low carbon structural steels to have higher yield strength and better toughness together with adequate level of ductility and good weldability.

Hall[2] and Petch[3, 4] demonstrated that ferrite grain refinement increases the yield strength and decreases the impact transition temperature. Initially, grain refining was done with aluminum and nitrogen through the formation of aluminum nitride precipitates[5, 6] Later, other additives such as vanadium, niobium and titanium were also shown to produce

grain refinement, but these particles responsible in this case were found to be the carbonitrides and also nitrides of vanadium, niobium and titanium[7]. The methodology of structure-property relationship developed by Pickering and Gladman[8] hastened the introduction of normalised grain refined steels These steels had yield strength 75 to 125 N/mm^2 higher than that of mild steel together with subzero impact transition temperatures.

Numerous studies were made on the effects of Cr, Ti, Nb and V additions on the structure and properties of low carbon structural steels[9-20]. The effects of small addition of vanadium on the structure and properties of low carbon structural steels are now well-established[10-17]. Precipitation effect of Nb on the strengthening of micro-alloyed steel was also studied[18, 19]. From the combined effect of Nb, V and Ti, Gawne and Lewis[20] found higher strength and ductility than plain carbon steel. Although studies were made on low carbon molybdenum steels but virtually a detailed study on the effect of small addition of molybdenum on the structure and properties of low carbon structural steels is not available. Current research[21,22] have shown that molybdenum improves the grain size and influences the transformation characteristics and properties of carburized steels. Nickel when added to steel remains in solution both in austenite and ferrite. It produces a solid solution strengthening effect. The effect of molybdenum in combination with nickel is not very clear.

The present work, therefore, will investigate the effect of small addition of molybdenum and nickel individually and in combination on the structure and properties of low carbon structural steels.

CHAPTER 2

HIGH STRENGTH, LOW ALLOY (HSLA) STRUCTURAL STEELS

2.1.Introduction

The development of high-strength low-alloy (HSLA) steels has included studies that considered the relationship between mechanical properties and microstructure[19, 23] Although the early HSLA steels were based on a ferrite-pearlite structure, the group now encompasses bainitic and martensitic structures[24] In recent years a number of studies have been carried out to determine the structure-property relationship in these steels[25, 26]. There are numerous existing and potential applications for high strength steels in the context of producing weight reductions in the construction (e.g. bridge, building etc.) line pipe, automotive, shipbuilding, power generation industries and packaging industries[20, 27-32]. The cost advantages vary with the end product, but in general, their high strengths allow a reduction in the thickness of engineering parts, enabling the user to purchase lower tonnage and this more than compensates for their additional unit costs[33, 34] High strength steel can also make a substantial contribution to energy efficiency. The motor car, in particular, is a voracious consumer of energy, and its improved fuel economy may be achieved either improving the operating efficiency of the engine or by a more efficient design of the vehicle weight. The use of high strength steels allows the body thickness and weight to be reduced, while maintaining equivalent dent resistance and effective dynamic elastic modulus[35, 36] The rapid acceptance of high strength steels compared with that of alternative weight saving materials (e g. aluminium

alloys, structural polymers), is a result of their low cost penalty per kilogram of weight saved and their relatively minor effect on existing manufacturing methods and facilities[29].

2.2. Requirements

Advances in engineering design have required the structural steels to have the following properties:

a. High yield strengths for greater load bearing capacity by lighter sections.
b. High degrees of toughness i.e. low impact transition temperature and high ductile shelf energy
c. Good weldability.
d. Good formability, especially in bending.
e. High level of ductility, i e. good fracture resistance in through thickness direction.

Up to present, the micro-constituents of structural steels are mainly ferrite and pearlite. However, acicular structure (bainite and low carbon martensite) is also useful when particularly high yield strengths are desired.

2.3. Factors Affecting Strength and Toughness of HSLA Steels

2.3.1. Ferrite Grain Size

The strength and toughness of high strength, low alloy (HSLA) structural steels with ferrite-pearlite structure are greatly influenced by ferrite grain size. Fine ferrite grains are beneficial for both yield strength and toughness[1-3, 32]. Pickering[33] has summarized the earlier developed quantitative relationships between micro-structural and compositional parameters and the mechanical properties of silicon-killed, carbon manganese steels, in the following two equations:

$$Y.S.\ (MN/mm^2) = 70 + 32[Mn] + 84[Si] + 680[P] + 30[Cr] + 33[Ni] + 11[Mo] + 38[Cu] + 5000[N] + 18\ 1d^{-1/2} \quad \text{----------(1)}$$

$$ITT(°C) = -19 + 44\times\%Si + 700\times\sqrt{\%N_f} + 2.2\times\%Pearlite - 11.51d^{-1/2} \quad \text{----------(2)}$$

where, N_f = the 'free' nitrogen content,

d = the ferrite grain size in mm and

ITT = Impact Transition Temperature

The compositions are expressed in weight percent.

From these equations it is evident that fine ferrite grains are beneficial in improving both yield strength and toughness while pearlite has a detrimental effect on the impact transition temperature. Increase in carbon content, i.e. pearlite impairs the toughness and reduces the charpy upper shelf energy[34]. Therefore, it is essential to have a low carbon content and to produce the finest ferrite grain size possible

A theoretical model for grain growth has been developed and the control of grain size in metals by second phase particles is well established. Grain growth involves an increase in the size of the grains with a corresponding decrease in the number of grains. The process therefore necessitates the disappearance of some grains, usually the smaller ones Small particles precipitated by prior treatment pin grain boundaries and retard grain growth during re-heat-treatment resulting in a relatively unchanged matrix, but overheating cause an abnormal type of grain growth resulting the growth of very few grains in a relatively unchanged fine matrix. This leads to the development of extraordinarily large grains, which may or may not be accompanied by some of the fine grains, which have not been consumed and retain their fine grain size. The models of grain control have been proposed by Zener, Paranjpe, Hillert, Webster and Gladman. These were fully reviewed by S. Nultawach[10] and Bepari[11] The current review will present a brief summary of the most recent theory of Gladman[35] in the light of ferrite grain control.

Refining the prior austenite grain size is the prerequisite for fine ferrite grains, because of ferritic nucleation on the austenite grain boundaries. Grain growth in polycrystalline materials occurs by grain boundary migration, which is discontinuous with respect to rate and direction[16]. Austenite grain growth can be inhibited by microalloying additions, which cause the presence of second phase particles in austenite.

These second phase particles occurring in the boundaries reduce the boundary area and therefore lower the driving force for grain growth. The presence of these particles dramatically changes the grain-coarsening characteristics due to their interaction with the austenite grain boundaries. These interaction results form the elimination of grain-boundaries area (energy) when the boundary intersects the second phase particles[36]. Any movement of the grain boundary away form the particle would result in a local energy increase and have a drag effect on the migrating boundary .The binding force between particle and boundary is greater than that available by thermal activation[37]. For a given volume fraction of pinning particles, the pinning energy is greater when the size of pinning particles is smaller and therefore there is a critical particle size below which pinning is effective[16] Consequently, energy for unpinning must be supplied from some other source, such as the energy release resulting from grain growth. Energy changes accompanying the migration of a pinned boundary[35] have shown that the criterion for unpinning can be expressed as:

$$r^* = \frac{6R_0 f}{\pi}\left(\frac{3}{2} - \frac{2}{Z}\right)^{-1} \text{ ----------(3)}$$

where,

R_0 = mean matrix grain radius

r^* = Critical particle radius defined by the activation energy barrier being reduced to a level at which thermally activated release occur

f = volume fraction of the precipitates

z = Ratio of the radii of larger grains and the matrix grains

It is relatively simple to convert the grain coarsening criterion into a form giving a critical number of particles, n_v^* of size r

$$n_v^* = (\frac{3}{2} - \frac{2}{Z})(\frac{1}{8} R_0)(\frac{4\pi}{3v})^{2/3} \text{ ----------(4)}$$

A critical particle radius, r*, can than be calculated from a knowledge of the volume fraction of the particles, the matrix grain radius, and the ratio of the radius of larger grain to that of its neighbours For most polygonal structures, experimental works suggest that a **Z** value of 1.5 would be reasonable. In equation (3) the critical particle radius increases as either the volume fraction of particles or to the matrix grain size increases. A very significant effect, which occurs in all metallic systems at elevated temperatures, is the coalescence of precipitate particles. The coalescence of precipitate particles is of special significance in view of the effect of particle size on the energy barrier, which opposes grain growth. When coalescence has permitted the particle size to reach the critical size r*, grain growth may occur, thus decreasing the energy of the system

Increasing the grain size heterogeneity decreases the critical particle radius. At some critical particle size, the driving force for grain growth equals to the pinning force exceeds the pinning force. Thus, fine particles are more effective than coarse particles in restricting grain growth. Since there is a critical particle size for a given volume fraction and grain structure, particle coarsening rather than reduced volume fraction by dissolution is preferred for grain growth under isothermal conditions. However, any increase in temperature causes some solution of the precipitates and the reduced volume fraction permits grains with a smaller **Z** ratio to grow, thus increasing the number of grains with are growing.

Alloying elements may interact with the mobility of austenite grain boundary and/ or the interfaces between the austenite and the growing products of austenite decomposition during the transformation not only as atoms in solid solution but also as precipitates[16]. In the normalized condition, austenite grain refinement may be achieved by pinning with precipitates of aluminum nitride or the carbonitrides of niobium, vanadium and titanium.

For effective pinning, the specific alloy addition must be selected to produce fine particles. A fine initial particle size is desirable to prolong the time taken for the particle to reach the critical particle size above which grain growth occurs. The ferrite grain size achieved by this method is ~5 μm. Depressing the transformation temperature, either by alloying additions or by increasing the cooling rate, is also widely used to give grain refinement provided acicular structure are not produced Controlled rolling techniques also give very fine grain size, possibly somewhat smaller than 5 μm.

2.3.2. Precipitation Strengthening

In steels the addition of small amounts of other metals have the effect of strengthening the ferrite matrix by formation of fine precipitates. The effectiveness precipitation strengthening from micro-alloying phase and its precipitation kinetics during cooling. Titanium, niobium and vanadium are the important alloy additions for precipitation strengthening. The strength rises mainly from the precipitation of nitrides, carbides and carbonitrides. Those precipitates of niobium and vanadium which are not dissolved during austenitising usually do not strengthen but cause grain refinement. On cooling, the already dissolved carbonitride will reprecipitate during and after ferrite transformation to give a rise in yield strength. Bepari[11] reported that vanadium carbide and vanadium carbonitrides are excellent precipitation strengtheners while aluminum nitride dose not produces any appreciable precipitation strengthening effect

The increase in yield stress due to precipitation strengthening arises principally from the direct interaction between dislocations and the distributed second phase particles. Orowan[38] explained the cause of the decrease of the yield stress when the critical particle size is exceeded. He showed that yield can occur without particle shear. To quantify this Orowan proposed a model, which is as follows. When a moving dislocation encounters second phase particles, it bows between them until it form a semi-circular shape the diameter of which is approximately equal to the spacing between the two surfaces. The dislocation configuration then becomes unstable and segments of the dislocation are

constrained to form a dislocation loop around each particle. The main dislocation is thus free to continue its passage through the lattice.

Orwan[38] showed that the yield strength of the alloy is the sum of the matrix flow stress τ_m and the resolved shear stress to bow dislocation between the dispersed particles, i.e..

$$Y.S. = \tau_m + \frac{2T}{bL} \text{----------(5)}$$

where, T =Line tension of dislocation .

b= barger's vector.

Later, using the approximation for the line tension of dislocation T= 1/2 Gb^2, Kelly and Nicholson[39] modified the Orowan equation to give .

$$Y.S = \tau_m + \frac{Gb}{L} \text{----------(6)}$$

where , G = shear modules of the matrix plane .

There is no question as to the validity of the Orowan bowing theory providing the following conditions are fulfilled. Firstly, dislocations are confined in their slip plane. Secondly, the particles are neither sheared nor fractured in the bowing process. Finally, the structural feature which control the matrix flow stress uniformly retards dislocation movement over distances which are large compared with L, the planer inter-particle.

Ashby[40] has proposed the most successful modification of Orowan model, which adopted some modified treatment on the line tension of dislocation . On the Ashby - Orowan , the line tension has been recalculated taking into account the effects of the character of the dislocation , scale of the bending and stacking fault or anti - phase boundary energy .

The result from the Ashby -Orowan model differs rather little from that of the original one. How ever, one major difference between the two models is that the Ashby-Orowan model predicts that the edge dislocation by - pass particles more easily than do screw dislocations, the original Orowan calculation predicts that the reverse is true.

This theory is considered very feasible because it has incorporated the models of Kocks[41] in

which the realistic, random particle distribution is assumed. The Ashby-Orowan model can be expressed quantitatively as follows.

$$\tau = \frac{1}{1.18}\left(\frac{1.2Gb}{2\pi L}\right)\ln\left(\frac{X}{2b}\right) \text{----------(7)}$$

where, τ = the resolved shear stress in N/mm^2

X = mean planar intercept diameter of a precipitate.

By putting the value of G and b for ferrite, 80300 N/mm^2 and 2.5 A^0 respectively, the equation becomes:

$$\tau = \frac{2.6}{L}\ln\left(\frac{X}{0\ 00025}\right) \text{----------(8)}$$

here l. and X are measured in μm.

Assuming that the yield stress increment due to particles is twice the resolved shear stress required to overcome their effect,

$$Y.S._p = \frac{5.2}{L}\ln\left(\frac{X}{0.00025}\right) \text{----------(9)}$$

Assuming that the particles are spheroidal so that their volume fraction can be given by.

$$f = n_s(\frac{\pi X^2}{4}) \text{ ---------- (10)}$$

where, n_s= the number of particles per area of the slip plane
then,

$$L = X(\sqrt{\frac{\pi}{4f}} - 1) \text{ ---------- (11)}$$

for relatively small fractions of fine precipitates formed in micro-alloying steels, L>>X, then

$$L = X(\sqrt{\frac{\pi}{4f}}) \text{ ---------- (12)}$$

The final expression of the yield strength due to precipitate can be written as:

$$Y.S._p = \frac{5.9\sqrt{f}}{X} \ln(\frac{X}{0.00025}) \text{ ---------- (13)}$$

Since 1/x is the predominant function of X, the stress increment due to fine precipitates increases in the precipitate fraction The close agreement between the observed increment predicted from the model implies that the increase in yield stress over that expected from grain size in the micro -alloyed steels is due entirely to the precipitation strengthening.

The cooling rate also controls the degree of precipitation A rapid cooling rate suppresses precipitation while a slow cooling rate allows the precipitation to over-age. In between, there is an intermediate cooling rate, which optimizes the precipitation strengthening. In general vanadium steels over-age more rapidly than niobium steels.

The intensity of precipitation strengthening is also very dependent on the steel with respect to the stoichiometric ratio, i e. the stoichiometric ratio of niobium and vanadium to carbon and nitrogen[42] The maximum temperature dependence of the solubility of the micro-alloying element carbonitrides occurs along the stoichiometric line and compositions on this line have the maximum potential for precipitation strengthening.

It is now clear that the toughness of high - strength, low alloy steels containing niobium is adversely affected by precipitation strengthening. Fine carbides of niobium and vanadium increase the impact transition temperature by about 0 3 to 0.5^0C for each N/mm^2 increase in yield strength by precipitation strengthening. This mechanism, therefore, that is considered viable only when strength levels above those attained within the practical limitations of ferrite grain refinement are needed.

2.3.3. Solid Solution Strengthening

Solid solution occurs when a mixture (or alloy) of two or more kinds of atoms is present in a crystal, usually with limited degree of solubility. Normally the solute atoms will have a different atomic radius from that of the solvent atom and these results in a misfit-giving rise to a localized distortion or strain in the crystal lattice Thus solid solution strengthening occurs as a result of distortion of the solvent lattice by the solute atom, causing an increase in the friction stress opposing dislocation movement. Solid solution strengthening effects are additive to yield strength. Solute atom such as phosphorus, nitrogen, manganese, silicon, carbon affect on solid solution strengthening, and consequently, on yield strength and tensile strength[20].

The following equations for the nominal yield strength σ_y (MNm^{-2}) and nominal tensile strength σ_t (MNm^{-2}), in terms of steel composition and grain size, were obtained from a statistical analysis of data[20]:

$$\sigma_y = 27 + 22d^{-1/2} + 165\times\%C + 470\times\%P + 3000\times\%N + 60\times\%Si - 665\times\%S \quad \text{----------(14)}$$

$\sigma_i = 150 + 16d^{-1/2} + 355\times\%C + 600\times\%P + 4505\times\%N + 77\times\%Si - 845\times\%S$ ----------(15)

where d represents the grain intercept length(mm) and the element concentrations are in weight percent. Equations (14) and (15) both explained 91% of the observed variations.

More approximate equations can be derived from the results when the grain-size data are omitted from the analysis. Such equations are useful in practice for a specified process route, when grain size is unknown and predictions of total strengthening effects of the elements are required. The total strengthening effect obtained from these equations is the strength increment produced by any grain-refining action of the element, in addition to its solution-hardening contribution - and its precipitation-hardening effect in the case of carbon. The following equations give the strength of the steels batch annealed at temperatures between 660 and 700°C, in terms of composition only:

$\sigma_y = 246 + 512\times\%C + 540\times\%P + 3935\times\%N + 68\times\%Si - 2174\times\%S$ ----------(16)

$\sigma_t = 292 + 563\times\%C + 678\times\%P + 5183\times\%N + 90\times\%Si + 18\times\%Mn - 1534\times\%S$ --------(17)

Equations (16) and (17) explain 72% and 83% of the observed variation, respectively. As indicated above, the concentrations of the elements affect the grain size, and this effect changes the values of the strengthening coefficients in equations (14) and (15).

Most solute atom particularly interstitial type (C and N_f) is detrimental to impact transition temperature (ITT). Manganese increases the strength and improves the toughness of the steel. Silicon has solid solution hardening effect in ferrite but has adverse effect on ITT. Silicon and manganese are both shown to be relatively weak strengthening elements[20]. Large concentrations of silicon and manganese are necessary to generate relatively small strength increases, and so these elements are not attractive strengthening options in sub-critically annealed steels[20]. Removal of free nitrogen

content of any steel decreases ITT and vice versa [43, 44] Nitrogen appears to be the most potent strengthener of all the elements investigated by D T.Gawne and G.M. H.Lewis and also produces steels with good formability in the as-annealed condition[20]. Phosphorus is an effective strengthening agent in steel, but excessively high phosphorus content can be detrimental to the product properties, in particular, contents above 0.1-0 2% The strengthening effect of carbon is relatively small and markedly depends on grain size[20]. The effect of sulfur is striking, as it is the only element that reduces the strength of annealed steel; a similar effect has been observed by Gladman et al[20].

2.4. Effect of Cooling Rate on Grain Size in a Carbon Steel

The principal of grain refinement by accelerated cooling can be explained by considering the effect of transformation temperature on the grain size of a new phase in an isothermal transformation. Diffusional phase transformations, such as ferrite transformation, proceed by nucleation and growth. When a parent phase transforms to a new phase, the grain size of the new phase is determined by the number of nucleation until the transformation is complete. Thus, with a large number of nucleation, the grain size of the new phase is small, and with a small number of nucleation, the grain size of the new phase is large[45].

Consider an isothermal transformation satisfying the following condition: nucleation occurs homogeneously, both nucleation and growth rates are constant with time, and grains grow spherically This type of transformation was originally treated by Johnson and Mehl. The total number of grains, **n** nucleated until the transformation is complete can be expressed as[45]

$$n = \int_0^\infty I_h \exp(-\frac{\pi I_h G^3 t^4}{3}) dt \cong 0.896(\frac{I_h}{G})^{3/4} \quad \text{----------(18)}$$

where I_h is the homogeneous nucleation rate per unit volume of matrix, G the growth rate and t time.

This calculation shows that the number of new grains is a function of the ratio of I_h/G. Since the grain size of a new phase is proportional to $n^{-1/3}$, the grain size of a new phase is a function of the ratio I_h/G. When the ratio I_h/G increases with a decrease in transformation temperature, the grain size of an isothermally transformation temperature.

In a transformation that involves continuous cooling, the transformation occurs in a certain temperature range and this range decrease with an increase in cooling rate Thus, for a transformation where the ratio of nucleation to growth rate increases with a decrease in temperature, the grain size of the new phase decreases with an increase in cooling rate Thus is why ferrite grains become refined by accelerated cooling.

A continuous cooling transformation can be considered as the sum of short-time isothermal holdings at successive temperatures. However, since ferrite nucleation and growth rates of ferrite are a function of an instantaneous temperature only, and not a function of thermal history On the basis of this assumption, the number of ferrite grains nucleated at temperature T_a during cooling n_a is given as

$$n_a = I_s(T_a)dt_a = -[\frac{I_s(T_a)}{Q(T_a)}]dT \text{ ----------(19)}$$

where $Q(T_a)(= dT/dt)$ is the cooling rate.

The growth rate of ferrite as a function of temperature can be obtained as follows. It is well established that the parabolic rate constant α for thickening is given by

$$\alpha = \frac{D^{1/2}(C_\gamma^e - C_0)}{(C_\gamma^e - C_\alpha^e)^{1/2}(C_0 - C_\alpha^e)^{1/2}} \text{ ----------(20)}$$

where D is the diffusivity of carbon in austenite, C_0 the initial carbon content, and C_γ^e and C_α^e the equilibrium carbon content in austenite and ferrite, respectively, which can be calculated by Hillert and Staffanson

The nucleation rate of ferrite I_α can be expressed as

$$I_s = (15/4)(\pi\alpha^3 t^{5/2} S_{gb}) \ln\left(\frac{1}{1-X}\right) \text{----------(21)}$$

where S_{gb} (= $4/\pi^{1/2}$ d_γ) is austenitic surface per unit volume, X the fraction transformed.

Ferrite grain size is proportional to $d_\gamma^{1/3}$ when austenite grain surfaces are the dominant nucleation site of ferrite. Thus, the theoretically estimated ferrite grain size can be expressed as a function of cooling and grain size as

$$d_\alpha = 1.0 q^{-0.17} d_\gamma^{1/3} \text{----------(22)}$$

The effect of increasing cooling rate is to increase the strength, decrease the ductility, and decrease the toughness. The increase in strength occur as a result of a decrease in proportion of ferrite and an increase in the amount others (e.g. pearlite or bainite)[46].

2.5. Ferrite Grain Size Dependence on Austenite Grain Size

In a polycrystalline material, nucleation is assumed to occur on four types of site, i.e. homogeneous sites and grain surfaces, edges, and corners[45]. The prior austenite grain size influences ferrite grain size influences ferrite grain size by nucleation site density. A ferrite grain size is proportional to $n_\alpha^{-1/3}$, where n_α is the number of ferrite grains nucleated until the transformation is complete per unit volume of austenite, and is proportional to nucleation site density. When ferrite nucleation occurs homogeneously in the austenite matrix, nucleation site density, and thus ferrite grain size, is independent of austenite grain size. When ferrite nucleation occurs at austenite grain surfaces, nucleation

site density is proportional to d_γ^{-1} since the grain surface area per unit volume is proportional to d_γ^{-1}. Thus, ferrite grain size is proportional to $d_\gamma^{1/3}$. When ferrite nucleation occurs at austenite grain edges, nucleation site density is proportional to d_γ^{-2}, since the grain edge length per unit volume is proportional to d_γ^{-2}. Thus, ferrite grain size is proportional to $d_\gamma^{2/3}$. When ferrite nucleation occurs at austenite grain corners, nucleation site density is proportional to d_γ^{-3} since the number of grain corners per unit volume is proportional to d_γ^{-3}. Thus, ferrite grain size is proportional to d_γ.

In summary, the dependence of ferrite grain size on austenite grain size is as follows: $d_\gamma^{1/3}$ for grain surface nucleation, $d_\gamma^{2/3}$ for grain edge nucleation, and d_γ for grain corner nucleation For homogeneous nucleation, ferrite grain size is independent of austenite grain size. In an actual ferrite transformation, several types of nucleation site act simultaneously, and the dependence of ferrite grain size on austenite grain size is a weighted average of the various nucleation modes.

2.6. Metallurgical Design of Ferrite-Pearlite steels

The metallurgical design of high strength, low-alloy steels with ferrite-pearlite structures require that compositional and microstructural parameters give the least increase in impact transition temperature per unit increase in yield strength, while maintaining adequate level of weldability and formability

Good weldability requires the steel to have a low hardenability that in turn is governed by the steel composition. A useful way of describing hardenability is to assess the total contribution to it of all the elements that are present. This is done by an empirical formula that defines s carbon equivalent (CE) value and takes account of the important elements that are known to affect hardenability. The formula most frequently used is:

$$CE = C + \frac{Mn}{6} + \frac{Cr + Mo + V}{5} + \frac{Ni + Cu}{15} \text{ - - - - - - - - - - - - - - - (23)}$$

An arbitrary CE value of 0.41 is specified above which welding may be hazardous. The equation points out the advantages of low-carbon, high-manganese contents.

There are four factors affecting the formability of ferrite-pearlite steels, namely: flow stress, work hardening and the total ductility prior to plastic instability, the first two properties should be low while the last two should be high.

Pearlite and refining the interlamellar spacing of pearlite increase both the flowstress and work hardening rate but reduce ductility[47]. Refining the ferrite grain size cannot offset the detrimental effect of pearlite but grain refinement is beneficial in terms of total ductility at fracture.

Non-metallic inclusions reduce the total ductility,[48,49] elongated inclusions are particularly detrimental to transverse ductility and upper shelf energy. Significant improvements in transverse ductility and upper shelf energy have been made in both plate and strip by reducing the volume fraction of inclusions or by inclusion shape control Inclusion shape is modified by adding elements such as titanium, zirconium or rare earth to replace the elongated inclusions by spherical one which may slightly reduce longitudinal ductility, but significant increases in both long - transverse and through thickness ductility occur.

Therefore, carbon and sulfur content should be low and the non-metallic inclusions should be uniformly distributed and shape-controlled in order to obtain good formability.

CHAPTER 3

EXPERIMENTAL PROCEDURES

3.1. Materials Preparation

Four different steels containing about 0.11% carbon were used in this experiment. The compositions of the steels are given in Table 1. The steels were made in an air induction furnace. All the melts were teemed at about 1600°C and produced cylindrical sound ingots. All the ingots were then rolled down to a size of about 16-mm in diameter. Steel 1 is the base steel with which the mechanical behaviour of other steels (2-4) containing Mo and Ni alone and in combination was compared.

3.2. Measurement of Prior Austenite Grains

In order to compare the properties of the four steels without any undue complication, each of the four steels should be heat-treated to a temperature, which would give the same austenite grain size. Attempts, therefore, were made to reveal the prior austenite grain boundaries at different austenitizing temperatures. Of the several techniques developed, the most satisfactory one is the developed oxidation technique[8] in revealing the prior austenite grain boundaries. However, considering the existing facilities available the isothermal transformation technique was followed to reveal the prior austenite grain boundaries of the steels

3.2.1. Isothermal Transformation Technique

This technique is based on the formation of a complete or nearly complete network of ferrite or iron carbide in the hypoeutectoid and hypereutectoid steels respectively. Steels with a carbon content remote from the eutectoid composition will reject, upon slowly cooling through the transformation range, either ferrite or cementite, depending upon the carbon content of the steel. The rejection of these constituents occurs largely at the prior austenite grain boundaries and under appropriate conditions, the constituents may be made to form a network around the original grains.

The steel specimens were heated to different austenitizing temperature, i.e. 900°C to 1150°C with intervals of 50°C. They were held at these temperatures for 45 minutes. After 45 minutes the specimens were transferred to a furnace at a temperature where ferrite rejection just takes place. This temperature was determined by trial and error was found to be 760-810°C. The specimens were held at the above temperature for 10 minutes. The specimens were then quenched in 10% brine solution.

The effectiveness of this process is not fare for Ni and Mo containing alloy steels, because at isothermal temperature fine ferrite grains would form instead of a complete or nearly complete ferrite network. Consequently, carburization technique was followed to reveal austenite grain boundaries

3.2.2. Carburization Technique

This technique is based on the formation of a continnous cementite network at the austenite grain boundaries. Carbon will diffuse in steel forming cementite at the austenite grain boundaries during austenitizing temperature. This cementite will form a continuous network around the original grains.

The steel specimens were heated to different austenitizing temperature, i.e. 900°C to 1150°C with intervals of 50°C. Before heating these specimens, they were packed in a

pot with carburizing mixture. Then they were placed in Blue-M furnace and the furnace was switched on After reaching the desired temperature, they were held at these temperatures for 1 hour and then cooled in this furnace to room temperature.

The assessment of austenite grain size was made from direct measurements of the austenite grains in the specimens under the optical microscope. The grain size was measured using the mean linear intercept method[50], counting grain boundary intersections with the circumference of the circle in the eyepiece of a microscope. The effective circumference of the circle was determined precisely by measuring its diameters with reference to a stage micrometer at the magnification used A total of at least 600 intersections were counted for each specimen. The grain size was then determined from this number.

The carburization technique was found troublesome in revealing the prior austenite grain boundaries for steels containing Ni and much time was spent in obtaining satisfactory results.

3.3. Determination of Heat-treatment Temperature

The heat-treatment temperature for each steel was determined by a careful examination of the austenite grain size. The criteria for the determination of the heat-treatment temperature for each steel were that the steels had the same austenite grain size and that the temperatures were such that an appreciable proportion of the solute elements had entered into solution for subsequent precipitation. An austenite grain size of 35 μm (Figure 3) was found to be suitable and the corresponding heat-treatment temperatures for steels 1-4 were 920°C, 1050°C, 1000°C, and 920°C respectively.

3.4. Heat-treatment of Specimens

The heat-treatments of the specimens were carried out in the Blue-M Silicon Carbide heat-treatment furnace. The steels were held at their respective heat-treatment temperatures for pre-selected periods. Then they were allowed to cool at four different cooling rates, namely: 120, 36, 12 and 3.6°C/min. These cooling rates correspond to the natural cooling through the transformation range of round bar with a diameter of 13, 50 120 and 380 mm respectively[50, 51].

3.5. Preparation and Mechanical Testing of Tensile Specimens

The heat-treated 13-15 mm dia bars were then machined into standard tensile specimens with a nominal diameter and a minimum parallel length of 3.99 and 22 mm respectively (BS 18). The tensile specimens were then tested with a tensile testing machine to obtain data on yield strength, ultimate tensile strength, % elongation and % reduction in area. A slide-caliper was used to measure the gauge length and diameter of specimens.

3.6. Optical Microscopy

Samples from the fractured tensile specimens were taken for microscopic examinations These samples were then ground, polished and etched in 2% nital. The microstructures of these specimens were then studied with the help of an optical microscope and photographs of the structure of each specimen were taken.

3.7. Determination of Ferrite Grain Size and Hall-Petch Plot

The specimens under optical microscope revealed ferrite and pearlite structure. Since the microstructure consisted of two phases, the assessment of ferrite grain size had to be done in two steps. First, the fictitious ferrite grain size was measured by the mean linear intercept method,[50] i.e. only the grain boundaries of ferrite were counted, and the pearlite

between two ferrite grains was considered as a common grain boundary. Second, the volume fraction of pearlite was estimated visually. Thirty to fifty fields were counted for each sample.

If the fictitious ferrite grain size is L, and the volume fraction of pearlite is 'v' then the true ferrite grain size 'd' is obtained by the following expression :

$$d = L\ (1 - v)$$

These measurements showed that although all the steels had started with the same austenite grain size, their subsequent ferrite grain size with a given cooling rate was different.

A Hall-Petch plot of yield strength vs $d^{-1/2}$ for each steel was drawn to obtain an idea how yield strength varied with the ferrite grain size.

CHAPTER 4

RESULTS

4.1 Prior Austenite Grain Size

The prior austenite grains of the steels were revealed by the carburization technique. The effectiveness of this method in revealing the prior austenite grain boundaries is shown in Figure 2. Although this technique proved troublesome for the steels containing Ni being presently studied, reasonably satisfactory results were obtained by trial and error.

The austenite grain size of the steels at different temperatures is listed in Tables 2-5 and plotted in Figure 3 where the 95 percent confidence limits for the grain sizes are indicated.

Austenite grain coarsened rapidly and linearly with increasing temperature when there were no particles to inhibit grain growth as in steel 1. The same trend was followed by steel 4. On the other hand, in steels 2 and 3 the austenite grain size remained very small in the temperature range over which precipitates were effective as inhibitors. However, as soon as the particles had lost their effectiveness, the grain-coarsening rate was then greater than that of the plain carbon steel. In steel 2, fine austenite grain size was observed compared with that in steel 3

4.2. Heat-Treatment Temperature

The heat-treatment temperature for each steel was determined by careful examination of the austenite grain size (Figure 3). The criteria for the determination of the heat-treatment temperature for each steel were that the steels had the same austenite grain size and that the temperatures were such that an appreciable proportion of the solute elements had entered into solution for subsequent precipitation. An adequate degree of solution is indicated by a marked increase in the austenite grain size. The austenite grain size of 35 μm was chosen to fit that criterion. The corresponding heat-treatment temperatures of the steels are listed in Table 6.

4.3. Optical Microscopy

The optical micrographs of all the steels at the four different cooling rates are presented in Figures 4-7. A visual comparison of the typical micrographs of Figure 4a and Figure 7a reveals that a faster cooling rate after austenitizing refines not only the ferrite grain size but also the pearlite size and distribution.

Optically it was found that all steels produced a polygonal ferrite-pearlite structure except steel 3 for cooling rates of 120°C/min and 36° C/min and steel 4 for the cooling rate of 120° C/min. For this fast cooling rate of 120° C/min, steels 3 and 4 gave a mixed structure of ferrite, pearlite and bainite. But the volume fraction of bainite in steel 4 was only small. Steel 3 also produced a mixed structure of ferrite, pearlite and bainite for the cooling rate of 36° C/min.

Some Widmanstatten ferrite-pearlite structure were observed along with polygonal ferrite-pearlite structure in steel 2 at the fast cooling rate of 120° C/min, in steel 3 at the cooling rate of 12°C/min and 3.6°C/ min and in steel 4 at all cooling rates except the slowest cooling rate of 3 6°C/ min. The volume fraction of Widmanstatten ferrite-pearlite in steel 3 at 3.6° C/ min was very small The presence of Widmanstatten structure/

bainite indicates that the transformation temperatures of steels 2-4 are lower than that of the plain carbon steel.

4 .4. Ferrite Grain Size and Hall-Petch Plot

The data from mechanical testing together with the pearlite volume fraction and the true ferrite grain size of the steels are presented in Tables 7-10. Using the values of yield strength and $d^{-1/2}$, a Hall -Petch relationship is plotted in Figure 9.

The steels started with a common austenite grain size, but their subsequent ferrite grain size under the same cooling conditions was not the same. This indicated that the precipitation kinetics and effectiveness in the control of ferrite grain size of Mo_2C and other factors were all different

CHAPTER 5

DISCUSSIONS

5.1. Prior-Austenite Grain Size

5.1.1. Isothermal Transformation Technique

This technique is based on the principle that ferrite or cementite precipitates preferentially at the prior austenite grain boundaries. Steels from austenitizing temperature when held for sometime at inter-critical temperature, will reject ferrite or cementite at the prior austenite grain boundaries. The volume of this ferrite or cementite is a function of inter-critical temperature and time at this inter-critical temperature.

The inter-critical temperature at which ferrite rejection begins was obtained for each steel by trial and error. Holding time at the inter-critical temperature to get a thin ferrite network around the prior austenite grain was also obtained in the same manner though it was very time consuming.

This technique worked well for steel 1, (plain carbon steel) at all temperatures. The effectiveness of this process for steel 1 in revealing the prior austenite grain boundaries is shown from Figure 1.

Problems were encountered with the determination of the inter-critical temperature and holding time for alloy steels. The Fe-Fe_3C phase diagram is altered by alloy additions and the extent of depression of the transformation region was not known. The

experiment had to be repeated many times to obtain both the inter-critical temperature and time at inter-critical temperature for getting reasonable ferrite network, around the prior austenite grains. But fine ferrite grains were observed instead of ferrite network around the prior austenite grains and it was difficult to count austenite grains. Therefore, this technique for measuring the austenite grain size was rejected and the carburization technique was adopted for this purpose.

5.1.2. Carburization Technique

This technique is based on the principle that carbon will penetrate through the prior austenite grain boundaries. Steels at the austenitizing temperature are held for sufficient time to allow diffusion of carbon as CO or C and then to form cementite net work along the prior austenite grain boundary. After annealing this structure will reveal cementite network around the pearlite that has transformed from austenite

This technique worked well for steel 1, (plain carbon steel) at all temperatures, but some problems were found to count prior austenite grains for Ni containing steels. Because nickel hinders to the penetration of carbon at the austenitizing temperature, accurate counting of austenite grain boundaries was difficult. So this grain size was measured by trial and error The effectiveness of this process for steels 1-4 in revealing the prior austenite grain boundaries will be evident from Figure 2.

5.1.3. Effect of Precipitates on the Prior Austenite Grain Size

The base steel 1, being plain carbon steel, does not contain second phase particles to inhibit grain growth. From Figure 3 it is evident that the austenite grain size of steel 1 increases linearly and rapidly with increasing temperature over the temperature range investigated. This is due to the free migration of grain boundaries to attain the equilibrium grain size when the temperature is raised. From Figure 3 it is evident that the austenite grain size of steel 4 increases linearly and rapidly as that of steel 1.

Steel 4 is basically steel 1 with nickel added to it. Nickel remains in solution in austenite at the austenitizing temperature and doesn't form any carbide particles So, there are no second phase particles to inhibit the growth of the austenite grains.

Second phase particles in the other steels pin the austenite grain boundaries, causing the steels to retain a fine grain size, which is almost unchanged during heating at successive high temperatures. However, as soon as the grain growth inhibitors begin to be ineffective at some elevated temperatures as a result of solution or coalescence, the grain-coarsening rate is then greater than that of steel 1. This is due to the fact that when the precipitates are no longer effective, the restricted grains want to achieve the equilibrium grain size as quickly as possible and thus cause an abrupt growth in the grain size.

Steel 2 produced the finest austenite grains at all temperatures. Steel 2 contains Mo_2C particles. These undissolved Mo_2C particles pin the austenite grain boundaries and inhibit the austenite grain growth at these temperatures resulting in fine austenite grains. These Mo_2C particles became ineffective at temperature above 1050°C resulting in large austenite grains as a result of coalescence and solution of Mo_2C.

Steel 3 contains both Ni and Mo. The grain coarsening behaviour was expected to be in between steel 2 and steel 4.This has been in fact, observed to be the case. Steel 3 produces finer austenite grain than steel 4 and coarser than steel 2. This clearly indicates that in the presence of nickel, Mo_2C is less effective in reducing the grain growth of austenite than Mo_2C in absence of nickel This may be thought to be due to the fact that the presence of nickel in steel alters the precipitation kinetics of Mo_2C in it

5.2. Effect of precipitate on Ferrite Grain Size

The mean ferrite grain size of the steels at four different cooling rates employed in the present experimental work is shown in Figure 8. It is evident from this figure that, although the steels had originally a common austenite grain size, the subsequent ferrite

grain size at the same cooling rate was not the same. This indicates that the precipitates in each steel influence grain refinement to differing degrees. It should be pointed out that the steels at the heat-treatment temperature contained some undissolved particles, the amount of which varied from steel to steel. It is possible that these particles may act as nucleation sites for ferrite and as obstacles in ferrite grain boundary migration, thus possibly significantly affecting the final ferrite grain size.

Steel 2 produced coarser grain size than plain carbon steel 1 and steel 3 produced finer grain size than steel 1, while steel 4 produced the finest grain size of all the steels at all the cooling rates.

It is fairly certain that the precipitations in steel 2 and steel 3 are essentially Mo_2C. The coarser ferrite grain size of steel 2 than of plain carbon steel 1 clearly indicates that Mo_2C does not produce any refinement of ferrite grain.

Steel 4 contains nickel. Nickel does not combine with carbon to form carbide particles. Nickel remains in solution in austenite. During cooling nickel depress the transformation temperature and hence ferrite transformation occurs from fine austenite grains. Fine austenite gives fine ferrite grains. The fine ferrite grain size in steel 4 is thus clearly produced from the fine austenite grain size caused by nickel in solution in austenite.

Steel 3 is basically steel 2 with nickel added to it i.e. it contains both molybdenum and nickel. The ferrite grain size of this steel 3 is expected to be in between that of steel 2 and steel 4. This has in fact been observed to be the case

5.3. The Hall-Petch Plot of the Steels

Using the values of yield strength and $d^{-1/2}$ in Tables 7-10, a Hall-Patch Plot of the steels is shown in Figure 9. Being plain carbon, steel 1 is anticipated to follow a straight line, which was in fact observed in experimental work. The relationship of yield strength and $d^{-1/2}$ was also found to linear for other steels. The linearity of steel 1 should be accurately

determined because steel 1 is used as the base steel with which the strength of the others is compared. The straight line through the data of steel 1 was drawn using the intercepts and slopes supplied by the standard method of least squares.

Steel 3 under the cooling rate of 120°C/min was found to contain a few ferrite and pearlite grains and was of mostly bainitic structure So it was not possible to measnre the ferrite grain size at this cooling rate. Steel 3 cooled at 36°C/min contain some Widmanstatten ferrite-pearlite structure. By neglecting the Widmanstatten ferrite-pearlite, it was possible to assess the ferrite grain size of the steel at these conditions by taking only the fields showing polygonal ferrite-pearlite structure. Steel 4 also contains Widmanstatten ferrite-pearlite structure at the cooling rate of 120°C/min. The ferrite grain size of this steel was also assessed in the same way. This procedure may give some error in the measurement of ferrite grain size at these cooling rates.

5.4. Yield Strength Increment from Precipitation Strengthening

The yield strength increment ΔYS is defined as the yield strength contributed by precipitation hardening. The yield strength increment of the steels at each cooling rate was determined and listed in Table 11 A plot of ΔYS versus cooling rate is shown in Figure 10. The results are obtained by subtracting the yield strength of the base steel at the same grain size from the observed yield strength of any other steel at each cooling rate.

It is evident from Figure 10 that ΔYS of steels 2-4 increases as the cooling rate increases ΔYS of steels 2 and 4 increases very slowly up to 36°C/min and then increases rapidly as cooling rate increases further. But ΔYS of steel 3 increases rapidly from cooling rate of 3.6°C/min to 12°C/min and maintains the same trend at higher cooling rates. The reason for this behaviour with these cooling rates of these steels may be explained as follows:

The strength increment due to precipitation increases with the reduction in precipitate size and the increase in precipitate fraction. A slow cooling rate allows the precipitates to become overaged and thus reduces their volume fraction resulting in lower strength increment.

It is evident from Figure 10 that steel 3 produced the highest ΔYS and steel 2 produced the lowest ΔYS of all the steels and steel 4 produced ΔYS higher than steel 2 and lower than 3. Steel 4 does not contain any precipitate. ΔYS of steel 4 is thus clearly due to solid solution strengthening caused by nickel.

Steel 3 contains both molybdenum as Mo_2C precipitates and nickel. The ΔYS of this steel is the combined effect of Mo_2C precipitate and solid solution strengthening caused by nickel.

It is thought that the presence of nickel in steel 3 alters the precipitation kinetics of Mo_2C. The much higher ΔYS of steel 3 than steel 4 or steel 2 is thought to be due to the finer dispersion of Mo_2C precipitate caused by the presence of nickel in it.

CHAPTER 6

CONCLUSIONS

6.1. Conclusions Drawn from the Present Work

(i) The isothermal transformation technique is not a satisfactory method for revealing the prior austenite grain boundaries in low carbon structural steels containing molybdenum and nickel.

(ii) The carburization technique is a reasonably satisfactory method for revealing the prior austenite grain boundaries in low carbon molybdenum structural steels.

(iii) On heating undissolved particles of molybdenum carbide, Mo_2C, refine the austenite grain size at temperatures below 1050°C, but the effect decreases with increasing temperature

(iv) Nickel does not produce any austenite grain refinement.

(v) In presence of nickel, particles of Mo_2C are less effective than Mo_2C particles in the absence of nickel in the refinement of austenite grain size. The precipitating particles of Mo_2C have no effect on ferrite grain size refinement.

(vi) The precipitating particles of Mo_2C have no effect on ferrite grain size refinement

(vii) Nickel refines the ferrite grain size.

(viii) Mo_2C precipitates increase the yield strength As the cooling rate increases, the yield strength increment (ΔYS) due to Mo_2C precipitates increases.

(ix) In the presence of nickel the contribution of Mo_2C to yield strength is more than that of Mo_2C in the absence of nickel.

(x) Nickel in solution contributes to yield strength.

(xi) Both molybdenum and nickel decrease the ductility of low carbon steel; but molybdenum is more harmful than nickel.

6.2. Suggestions for Further Work

(i) A study on the toughness of the steels should be carried out.

(ii) The precipitates of each steel should be studied by electron microscope. This will elucidate the effects of precipitate size, distribution and volume fraction

(iii) The effects of Mo_2C precipitates on the ductility of the steels should be studied in detail.

(iv) The effect of nickel on the increment of the yield strength due to solid solution strengthening is not well understood. A detailed investigation is, therefore, required.

REFERENCES

1 Bhole, S.D. and Billingham, J., September, 1983, Metals Technology, 10, 363
2. Hall, E.O., 1951, Proc. Pjys. Soc., Series B, 64, 747.
3. Petch, N.J , 1953, J.I.S.I , 174,25
4. Petch, N.J., 1959, SWAMPSCOTT CONF., M.I.T. Press, p 54
5. Wiester,H.J., Vogels, H.A. and Ulmer, H., 1959, Stahlund Eisen, 79,No. 16, 1120.
6. Preston, S., Hale, G. and Nutting, J., March, 1985, Materials Science and Technology, 1, 192.
7. Chen, Z., Loretto, M.H. and Cochrane, R.C., October, 1987, Materials Science and Technology, 3, 836
8. Pickering,F B and Gladmam, T., 1963, " Metallurgical Development in Crbon Steels", I.S.I. Special Report, No. 16,1120.
9. Irvine, K.J., Pickering, F.B., and Gladman, T , 1967,J.I.S.I., 205,161.
10. Niltawach,S ,1977, ph . D. Thesis, University of Sheffield, U.K.
11. Bepari, M M.A., 1981, ph. D. Thesis, University of Sheffield, U K.
12. Bepari, M. M. A., jan, 1989, Metallurgical Transactions A, (20A), 13.
13. Bepari, M.M.A., jan. 1989, Materials Science and Technology, (5), 13.
14 Bepari, M.M.A..1990, Materials Science and Technology, in press
15 Webster, D , and Woodhead, J. H , December 1964, J I S. I P. 987
16 Garbarz, B and Pickering, F.B., November, 1988, Materials Science and Technology, 4, 967
17. Jaiswal, S. and Melvor, I.D., April, 1985, Materials Science and Technology, 1. 276.
18. Guimaraes, J.R.C. et al. January, 1984, 11, 13.
19. Heisterkamp, F. and Hulka. K., December. 1984, Metals Technology, 11, 535.
20. Gawne, D.T. and Lewis, G.M.H., March, 1985, Materials Science and Technology, 1, 184-187.
21. Sorowordi, K.M., M. Sc. Engineering Thesis, 1998, Dept. of Materials and Metallurgical Engineering, BUET, Dhaka
22. Sorowordi, K.M. and Bapari, M.M.A · Proc. of the Intl. Conf. On "Structure, Processing and Properties of Materials, SPPM'97", held in BUET, Dhaka, 15-17 November, 1997, pp. B62-B72Shams, 1985, Materials Science and Technology, (1), 950.
23. Haque, M.Z., 1989, M.Sc. Thesis, Bangladesh University of Engineering & Technology, Dhaka.
24. Reuben, R L. and Baker, T.N., January, 1984, Metals Technology, 11,6.
25 Deb, P. and Chaturvedi, M.C , May, 1983, Metals technology, 10, 167.
26 Mintz, B., February, 1984, Metals technology, 11, 52
27 Ridley, N., Maropoulos, S and Paul, J.D.H., March, 1994, Materials Science and Technology, 10, 239.
28. Walter, G H. , 1977, 'Microalloging' 75' , 622, Union Carbide Corp., New York.
29. Beardmore, P., 1981, Mater, Eng , (2), 250.

30. Haberfield, A.B. and Hudd, R C., 1982, Metall. Mater. Technol., (14), 405.
31. Zub, L. and Colello, A., 1980, SAE Reprint 800215, Society of Automotive Engineers, Dearborn, Mich.
32. Sage, A.M., June, 1983, Metals Technology, 10, 224
33. Pickering, F.B., October 1975, Microalloying 75 Symposium, Washington D. C , p 3.
34. Gladman, T., Mcivor, I D and Pickering, F.B., 1972, J.I.S.I.,(210), 916. Chambers, A.R. and Whittaker, D., August, 1984, Metals Technology, 11, 323.
35. Gladman, T., 1966, Proc. Roy. Soc. , Series A, (294), 298.
36 Smith, C.S.,1948, Trans, Met. Soc. A.I.M.M.E., 175, 1.
37 Mclean, D , 1957 ,"Grain Boundaries", London (Oxford University Press), p. 241 Senevirathe, G., 1983, Development Forum , Business Edition, 131.
38. Orowan , E., 1948, Symposium on Internal Stresses in Metals and Alloys, Institute of Metals, p.451.
39 Kelly, A. and Nicholson, R B., 1963, Progress in Material Science, (10), No. 3, New York (Macmillan.)
40. Ashby,M.F.. 1966, "Oxide Dispersion Strengthening", A I.M .M .E Conference, New York, p 143
41. Kocks, U.F.,1966, Phil. Mag., 13, 541.
42. Pickering, F.B.,1970,J .I.S.I.,208, 717.
43. Mackenzie, I.M.,1963, "Metallurgical Developments in Carbon Steels". I S.I., Special Report No 81,p 30
44. Smail, J.S , Keown, S R and Erasmus, L.A., 1976, Metals Technology Journal,April, p 194.
45. Umemoto, M, Guo, Z.H. and Tamura, I., April, 1987, Materials science and Technology, 3, 249.
46. Idemetor, U.A. and Hawkins. D.N , Sepember, 1988, Materials science and Technology, 4, 786.
47. Gladman, T., Holmes, B. and Pickering, F B., 1970, J.I.S.J. 208, 173.
48. Gurland, J., and Plateau, J , 1963, Trans A S.M.,56, 442.
49. McClintock, F.A., 1968, "Ductility", A.S M. Seminar Volume, Metals Park, Ohio, p 255.
50. Bepari, M.M.A., 1978, M Met Thesis, University of Sheffieeld, U.K
51. Headridge, J. B.,Keown, S.R. and Vergnano, P.A ,1978, Analytica Chimica Acta,98,157
52. Phillips, R., and Chapman, J.A., 1963, "Metallurgical Developments in Carbon Steels", ISI Special Report No. 81, p. 60.
53. Gladman, T., Dulieu, D. and Mcivor, I.D , October 1975, Microalloying 75 Symposium, Washington D.C., p. 25

Table: 1. Chemical Composition of Steels 1 to 4, wt.%

Steel No.	C	Si	Mn	S	P	Mo	Ni
1	0.10	0.28	1.18	0.021	0.028	-	-
2	0.12	0.20	1.10	0 022	0.022	0.31	-
3	0.11	0.29	1 27	0.025	0.025	0.30	1.10
4	0.13	0 16	1.40	0.027	0.038	-	1.26

Table: 2. The Prior Austenite Grain Size of Steel 1.

Temperature °C	PriorAustenite Grain Size µm
900	31
950	45
1000	62
1050	76

Table: 3. The Prior Austenite Grain Size of Steel 2.

Temperature °C	Prior Austenite Grain Size µm
900	24
950	26
1000	30
1050	35
1100	45

Table: 4. The Prior Austenite Grain Size of Steel 3.

Temperature °C	Prior Austenite Grain Size µm
900	25
950	29
1000	35
1050	45
1100	63

Table: 5. The Prior Austenite Grain Size of Steel 4.

Temperature °C	Prior Austenite Grain Size µm
900	32
950	44
1000	60
1050	74

Table: 6. Heat Treatment Temperature of Steels 1to 4.

Steel No.	Heat Treatment Temperature ^{0}C
1	920
2	1050
3	1000
4	920

Table: 7. Steel 1, Heat-Treatment Temperature 920^{0}C

Cooling Rate ^{0}C/min	Ferrite Grain Size, d (mm)	$d^{-1/2}$ $(mm)^{-1/2}$	Y.S. N/mm^2	U.T.S. N/mm^2	EL%	R of A%	Pearlite%
120	0.0143	8.35	301	452	36	78	12
120	0.0146	8.25	297	454	36	78	12
36	0.0166	7.75	279	436	35	76	10
36	0.0173	7.60	269	429	34	79	10
12	0.0121	6 85	250	421	31	74	8
12	0.0210	6.90	251	427	32	74	8
3.6	0.0235	6.52	246	421	33	76	8
3.6	0.0237	6 50	245	413	32	77	8

Table: 8. Steel 2, Heat-Treatment Temperature 1050^{0}C.

Cooling Rate ^{0}C/min	Ferrite Grain Size, d (mm)	$d^{-1/2}$ $(mm)^{-1/2}$	Y.S. N/mm^2	U.T.S. N/mm^2	EL%	R of A%	Pearlite%
120	0.0158	7.95	352*	538	23	65	25
120	0.0162	7.85	346*	522	22	57	25
36	0.0193	7.20	316*	524	11	68	20
36	0.0196	7.15	306*	496	33	68	20
12	0.0219	6.75	291*	499	24	62	17
12	0.0226	6.65	284*	485	24	54	17
3.6	0.0260	6.20	269	467	28	61	15
3.6	0.0269	6.10	266	467	30	62	15

* 0.2% Proof stress

Table: 9. Steel 3, Heat-Treatment Temperature 1000^{0}C.

Cooling Rate ^{0}C/min	Ferrite Grain Size, d (mm)	$d^{-1/2}$ $(mm)^{-1/2}$	Y.S. N/mm^2	U.T.S. N/mm^2	EL%	R of A%	Pearlite%
120	-	-	548*	693	19	65	-
120	-	-	552*	722	17	64	-
36	0.0158	7.95	511*	673	18	68	30
36	0.0164	7.80	481*	660	23	67	30
12	0.0190	7.25	454*	643	20	66	27
12	0.0185	7.35	476*	647	24	65	27
3.6	0.0233	6.55	390*	574	24	62	25
3.6	0.0226	6.65	390*	574	28	65	25

* 0.2% Proof Stress

Table: 10. Steel 4 (Ni), Heat-Treatment Temperature 920°C.

Cooling Rate °C/min	Ferrite Grain Size, d (mm)	$d^{-1/2}$ $(mm)^{-1/2}$	Y.S. N/mm^2	U.T.S. N/mm^2	EL%	R of A%	Pearlite%
120	0.0113	9.40	469*	635	24	65	25
120	0.0121	9.10	458*	618	16	38	25
36	0.0135	8.60	412*	598	25	70	23
36	0.0142	8.40	407*	588	24	69	23
12	0.0173	7.60	339*	596	25	65	23
12	0.0164	7.80	378*	562	21	58	23
3.6	0.0213	6 85	354*	559	29	62	20
3.6	0.02261	6.65	345*	556	33	73	20

0.2% Proof Stress

Table: 11. ΔYS of Steels 2 to 4.

Steel No.	Cooling Rate °C	Mean YS N/mm^2	Mean $d^{-1/2}$ $(mm)^{-1/2}$	ΔYS N/mm^2
1	120	298	8 30	-
2	120	347	7 90	77
3	120	-	-	-
4	120	469	9 25	144*
1	36	270	7 67	-
2	36	306	7.17	51
3	36	495	7 87	210
4	36	412	8.50	102*
1	12	250	6 88	-
2	12	290	6.70	45
3	12	450	7.30	185
4	12	370	7.70	85*
1	3.6	245	6.30	-
2	3.6	268	6.15	43
3	3.6	390	6.60	150
4	3.6	350	6.75	80*

* ΔYS of steel 4 is the yield strength increment due to solid solution strengthening.

(a) Steel 1

(b) Steel 4

Figure 1. Optical micrographs showing the prior austenite grain boundaries revealed by isothermal transformation technique, × 200:
(a) Steel 1, austenitized at 950°C
(b) Steel 4, austenitized at 1000°C

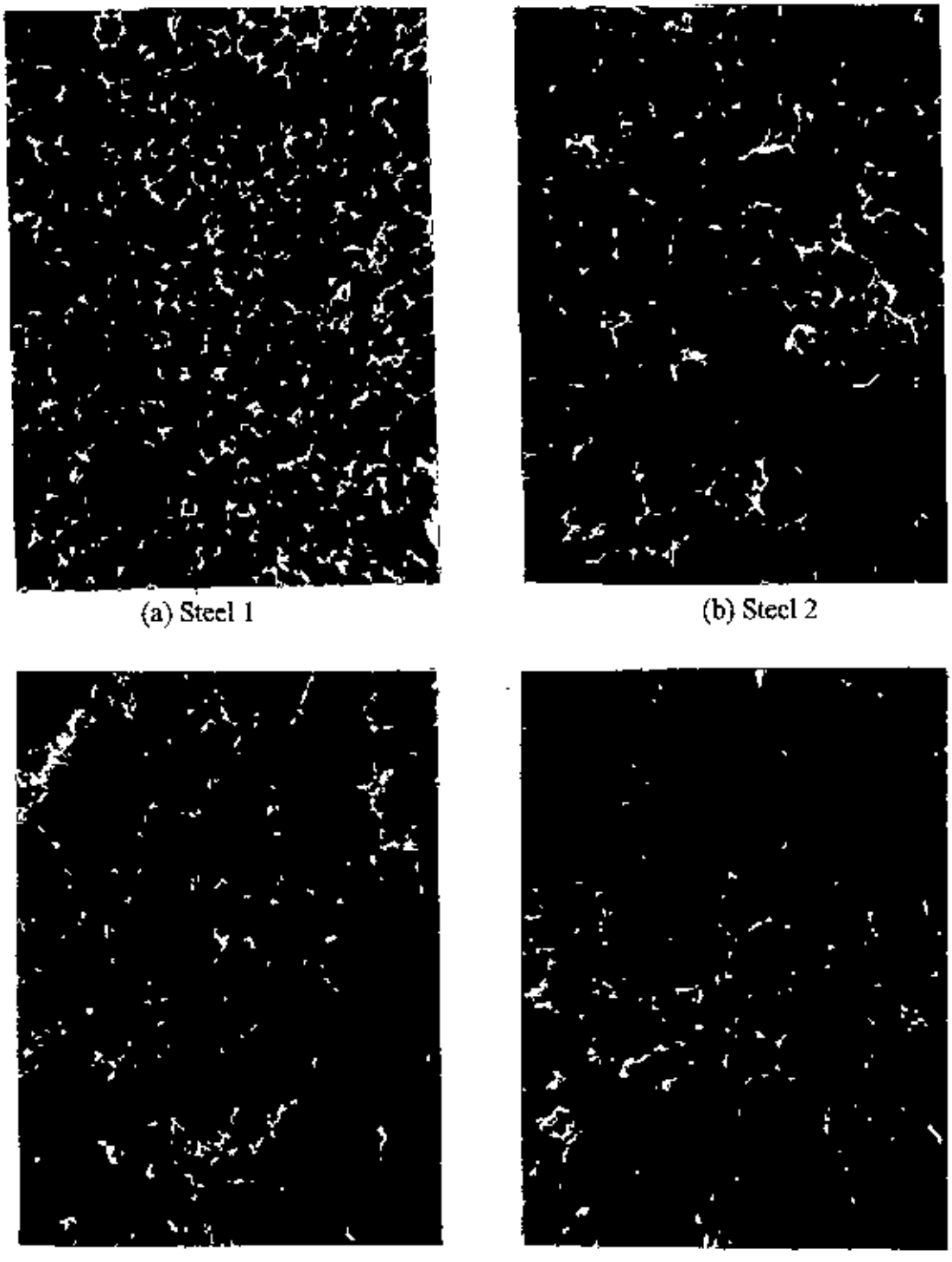

(a) Steel 1 (b) Steel 2

(c) Steel 3 (d) Steel 4

Figure 2: Optical micrographs showing the prior austenite grain boundaries revealed by carburization technique, × 200:
(a) Steel 1, austenitized at 900°C, (b) Steel 2, austenitized at 1100°C
(c) Steel 3, austenitized at 1000°C, (d) Steel 4, austenitized at 950°C

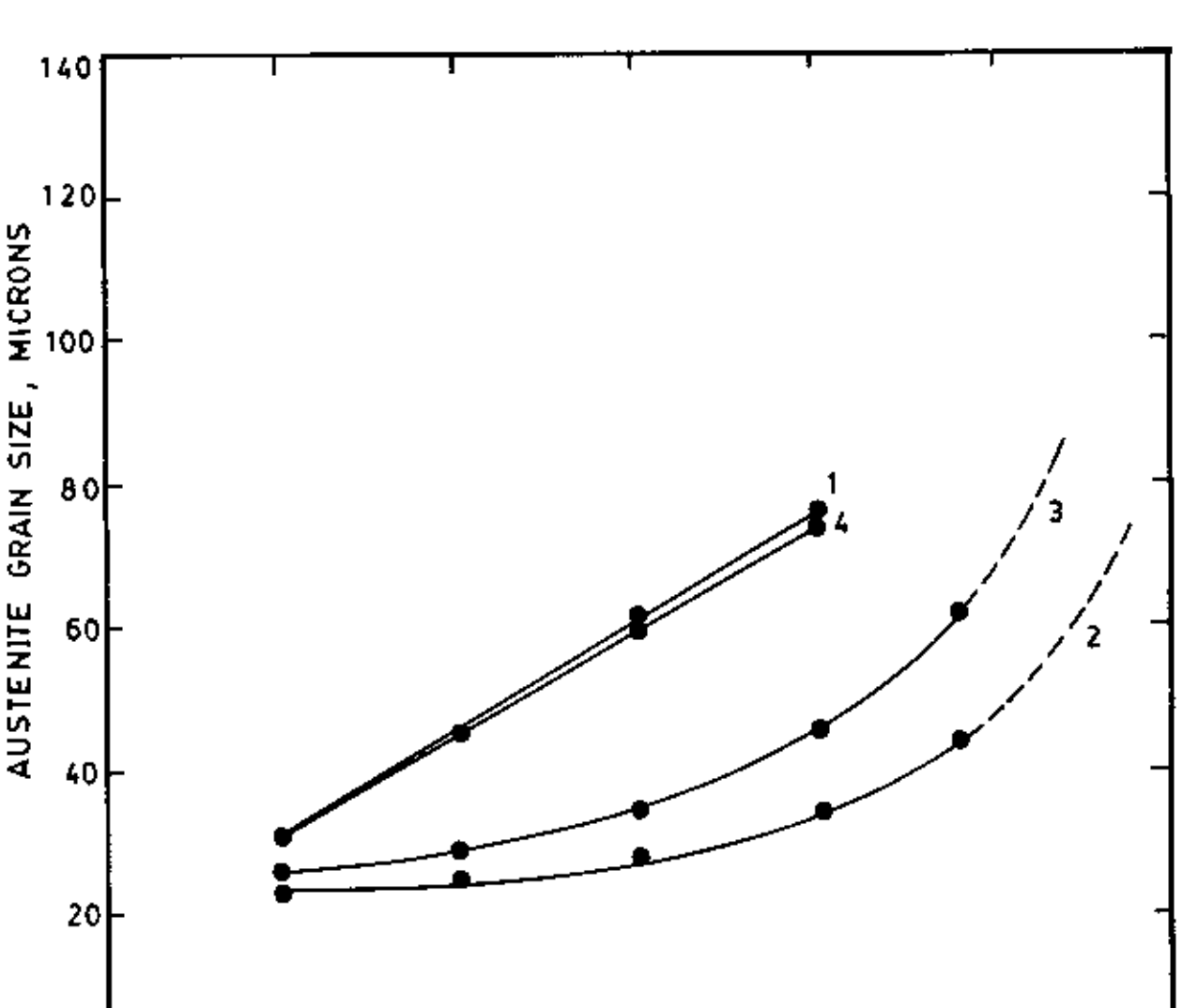

Figure 3: The variation of prior austenite grain size with temperature in steels1 to 4, error bars also incorporated.

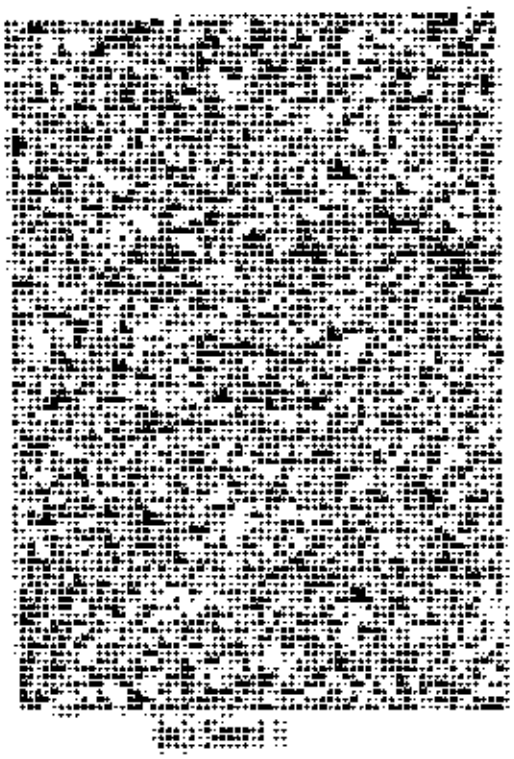

(b) Steel 2

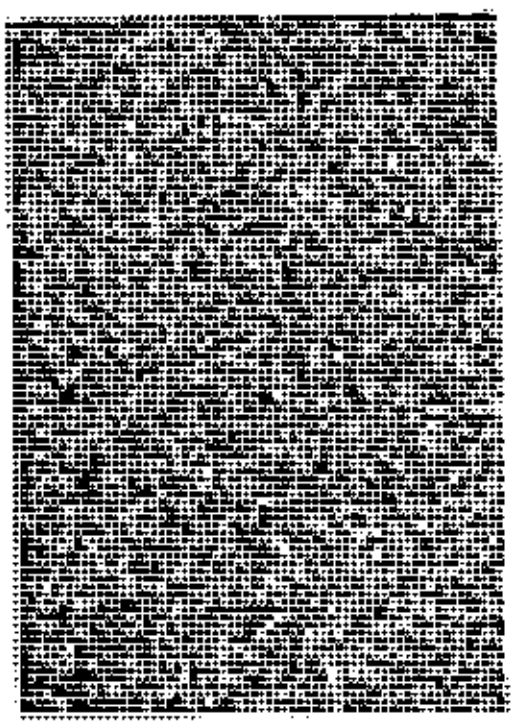

(c) Steel 3

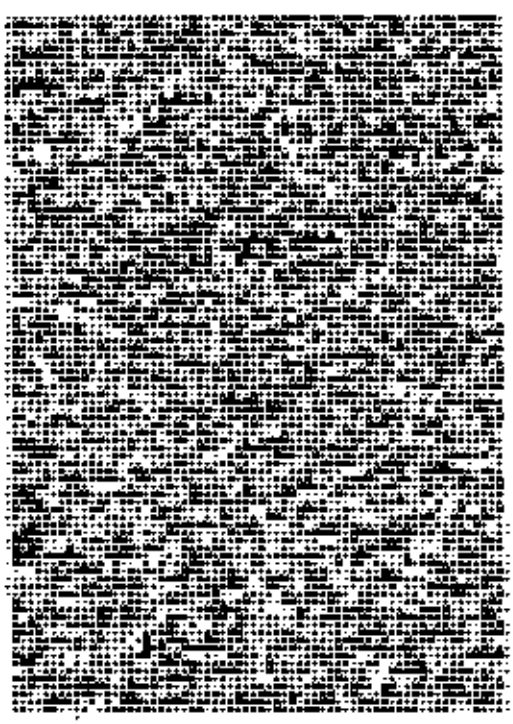

(d) Steel 4

Figure 4: Optical micrographs of steels 1 to 4 cooled at 120°C/min, × 200.

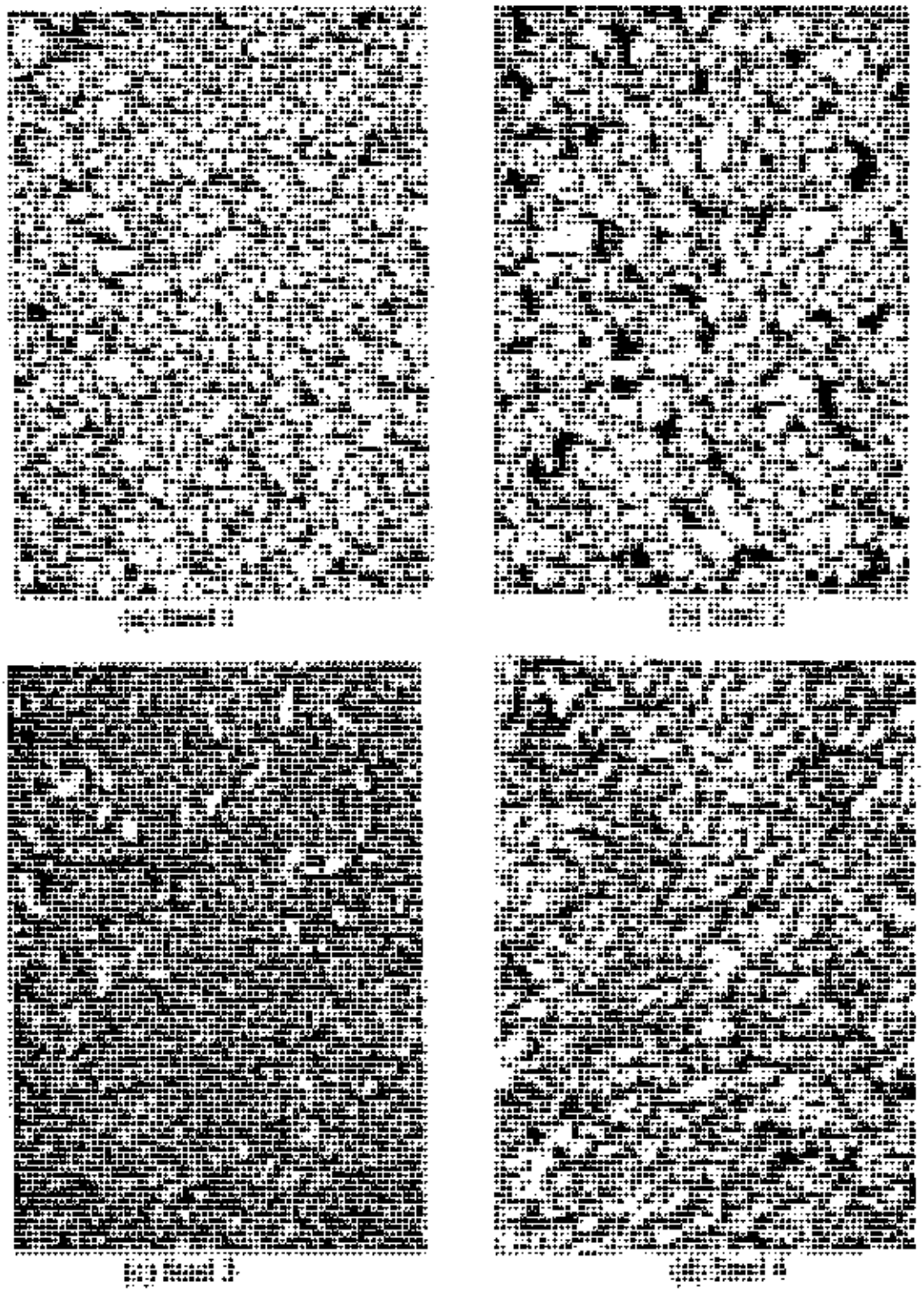

Figure 5: Optical micrographs of steels 1 to 4 cooled at 36°C/min, × 200.

(a) Steel 1

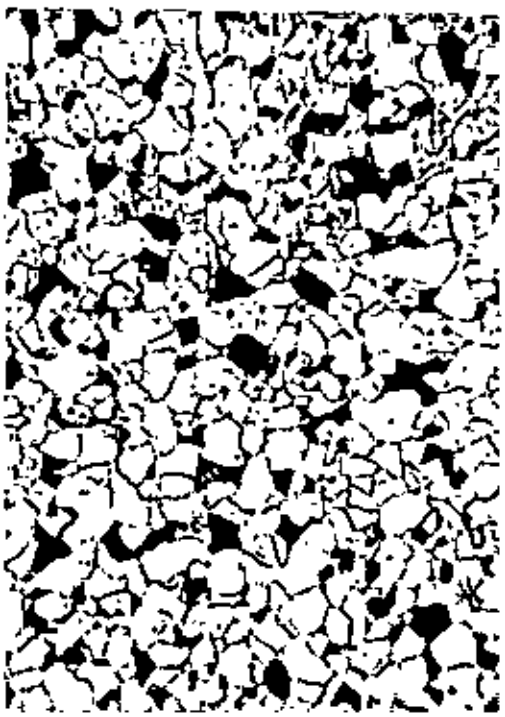

(b) Steel 2

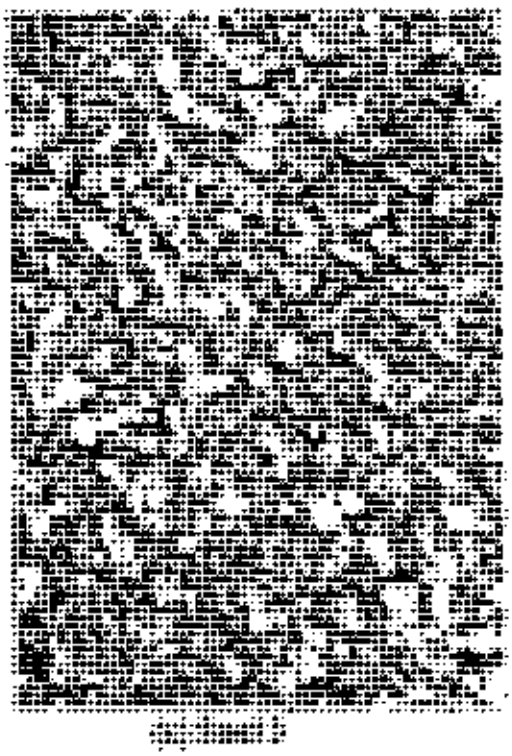

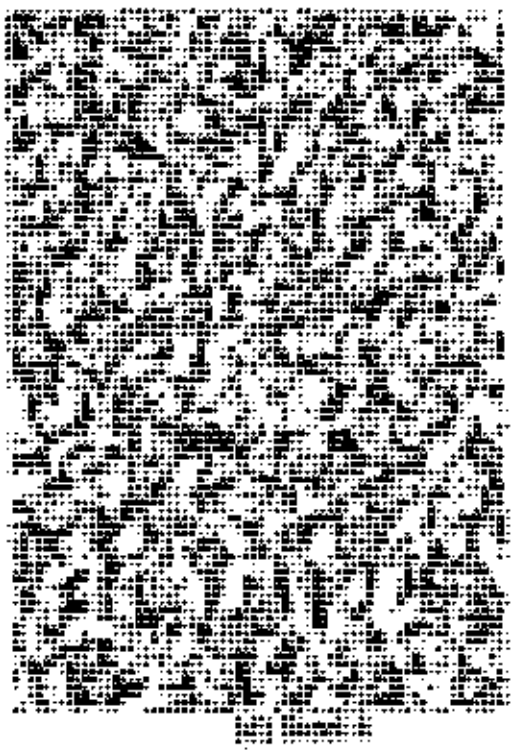

Figure 6: Optical micrographs of steels 1 to 4 cooled at 12°C/min, × 200.

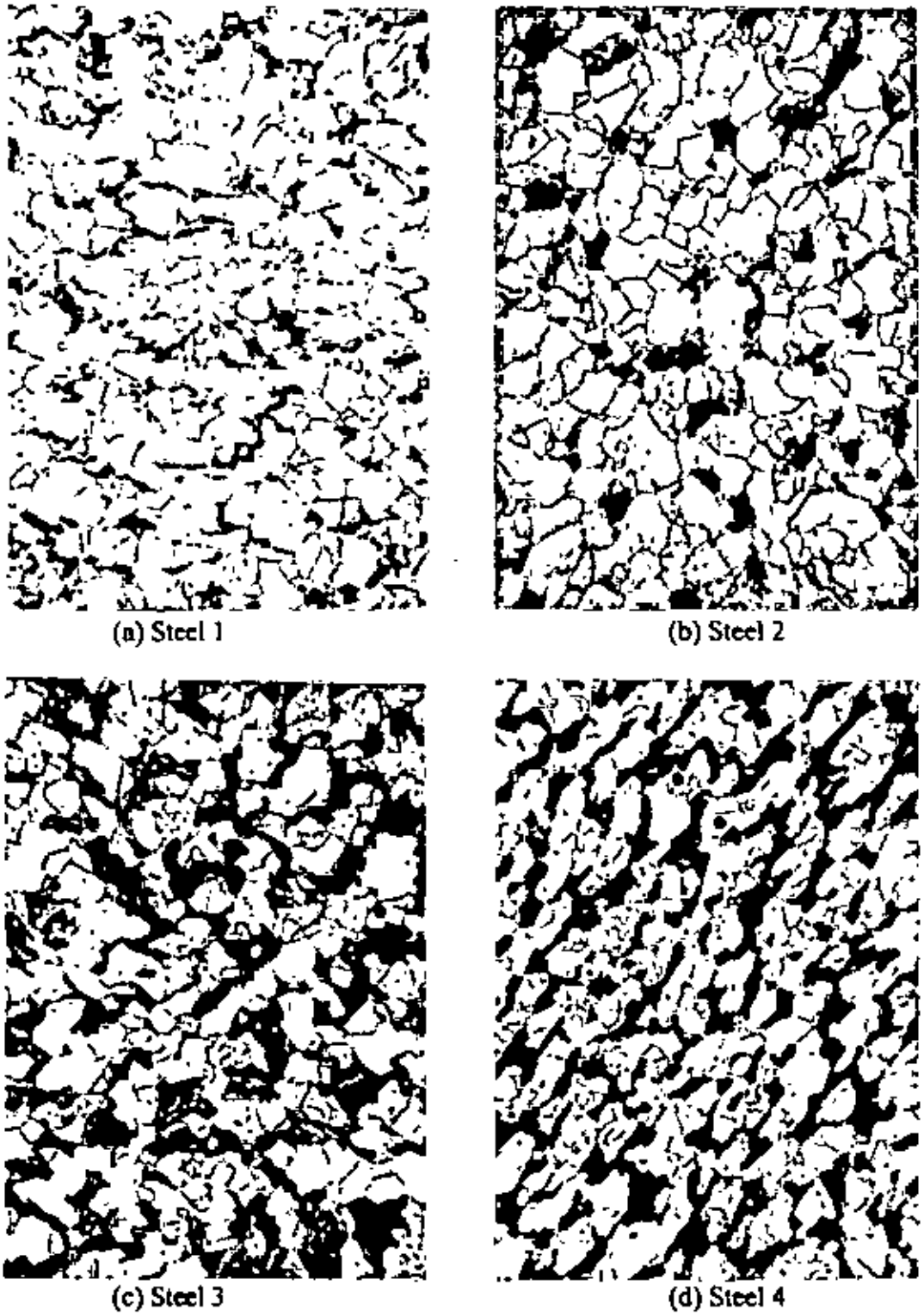

Figure 7: Optical micrographs of steels 1 to 4 cooled at 3.6°C/min, × 200.

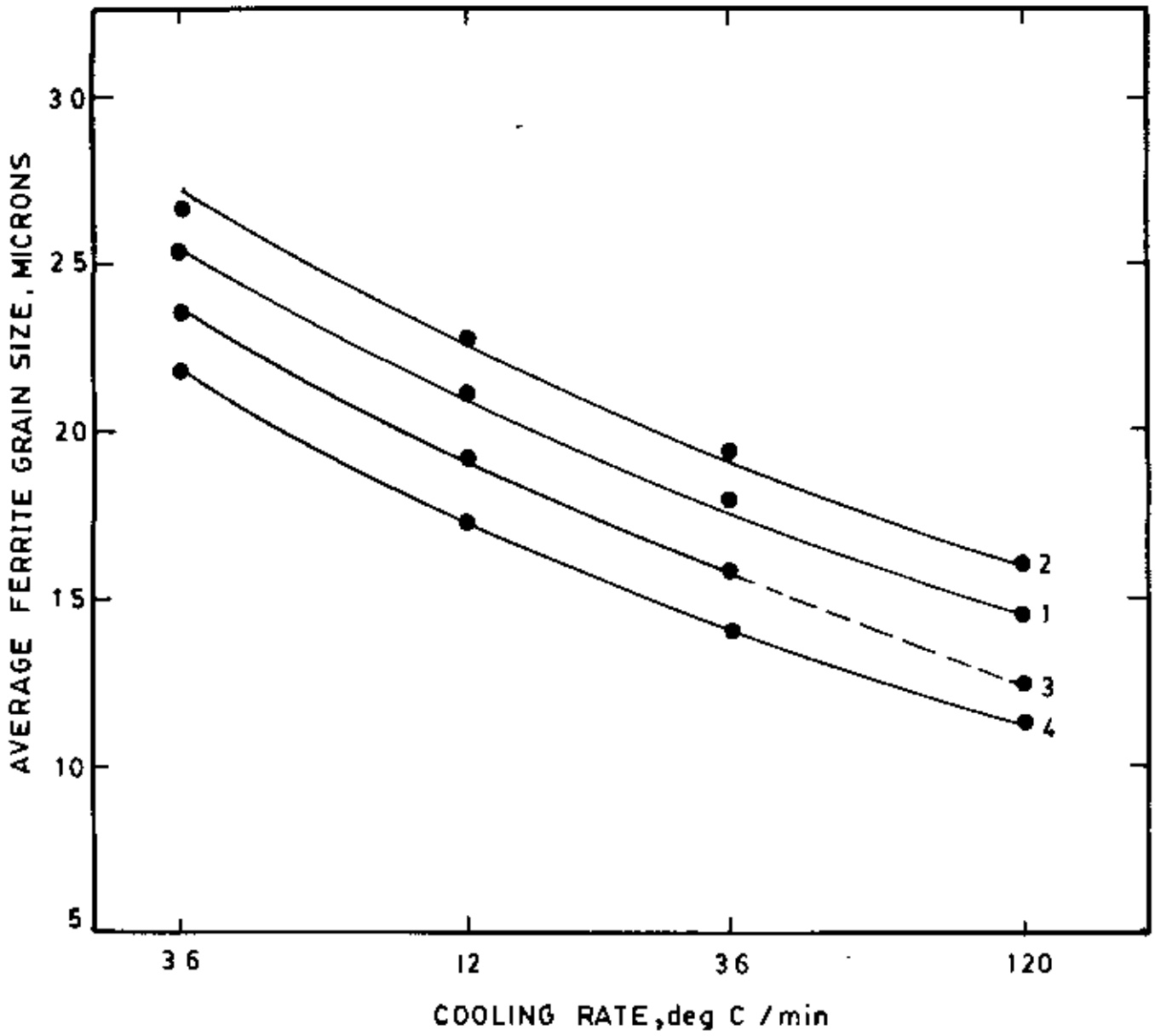

Figure 8: The ferrite grain size of steels 1 to 4, cooled at four different cooling rates from a common austenite grain size of 35 μm

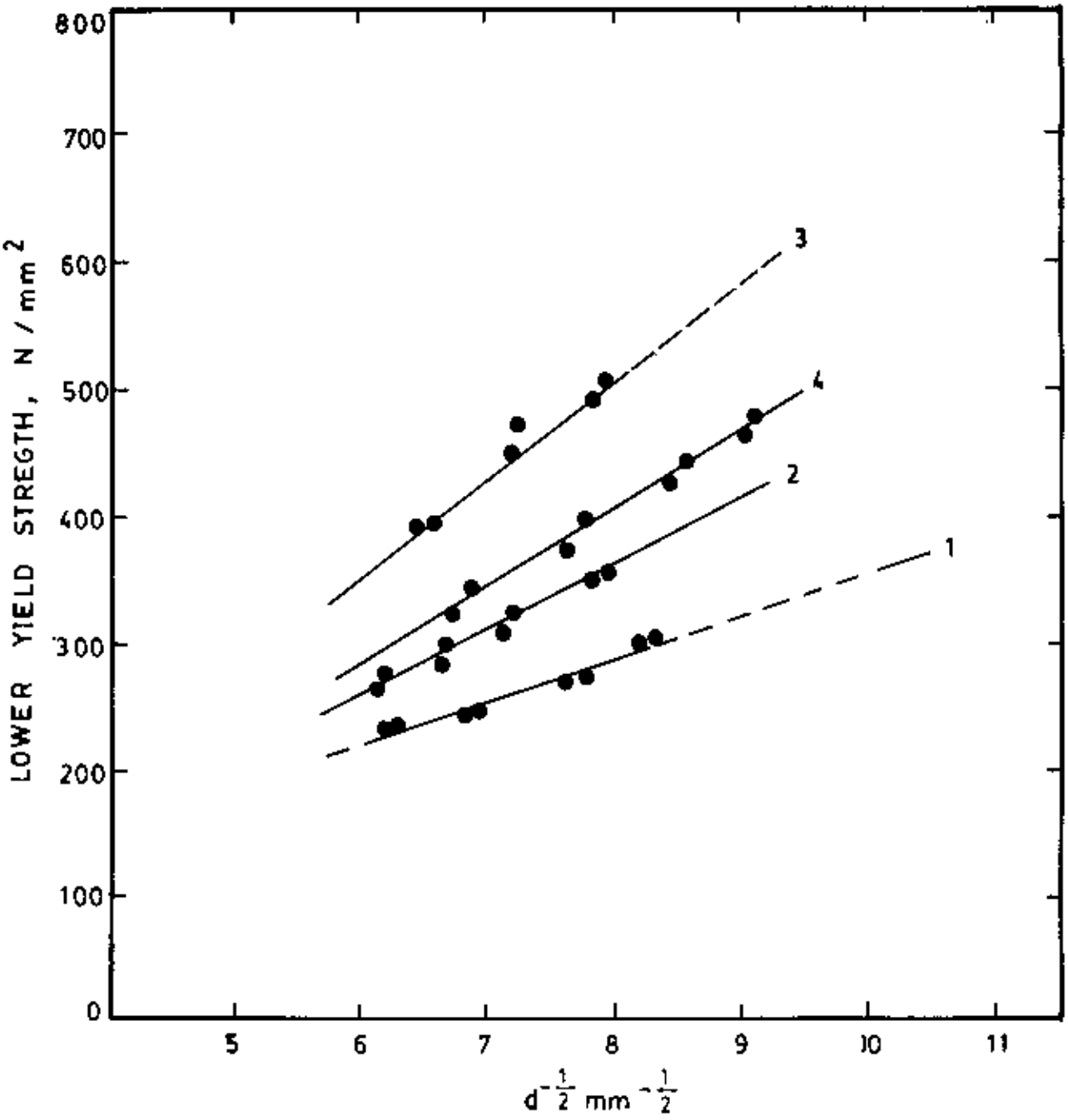

Figure 9: The Hall-Patch Plot of steels 1 to 4.

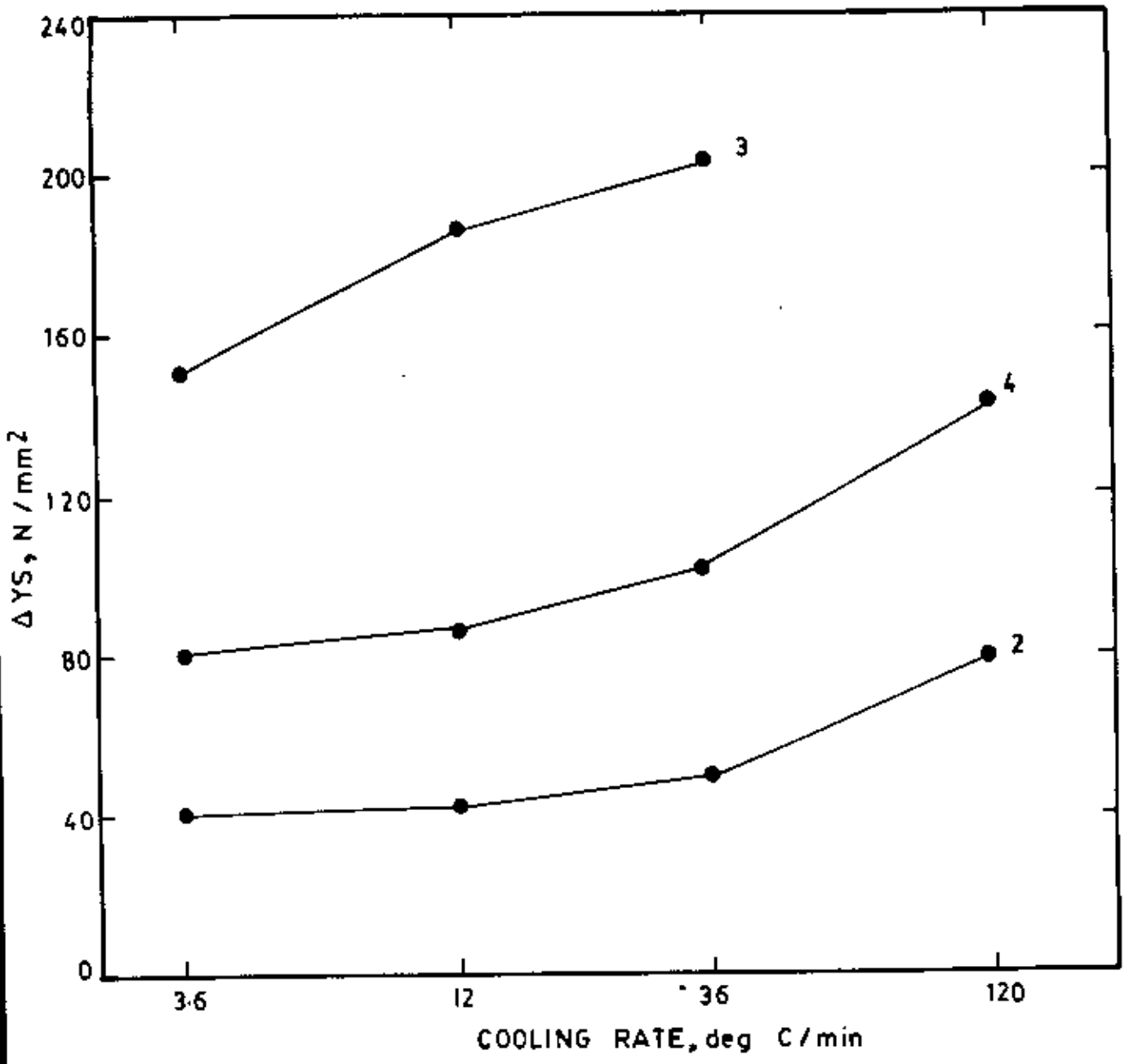

Figure 10: The variation of strength increment due to precipitation with cooling rates in steels 2 to 4